Journal of Materials Chemistry C

Accepted Manuscript

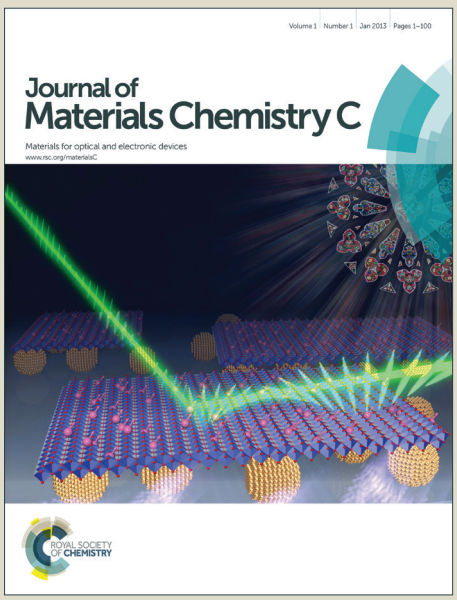

ROYAL SOCIETY OF CHEMISTRY

www.rsc.org/materialsC

Cite this: DOI: 10.1039/c0xx00000x

www.rsc.org/xxxxxx

ARTICLE

Water Induced Zinc Oxide Thin Film Formation and its Transistor Performance

Jingjing Chang,[a] Kok Leong Chang,[b] Chunyan Chi,[a] Jie Zhang,[b,*] Jishan Wu[a, b,*]

Received (in XXX, XXX) Xth XXXXXXXXX 20XX, Accepted Xth XXXXXXXXX 20XX
DOI: 10.1039/b000000x

This study reports the effect of water on the formation of zinc oxide (ZnO) thin film and the performance of ZnO thin film transistor (TFT). A systematic study is designed to reveal the structure-property relationship of this promising metal oxide semiconductor for high performance TFT at low processing temperatures. It is found that incorporating water molecules, either water vapor annealing or as an additive in the ZnO precursor, improves the formation of ZnO thin films as semiconductor with evident of higher TFT mobility (μ) and lower threshold voltage (V_T) shift. On the other hand, excessive amount of water in the ZnO precursor serves as acceptor-like traps in the ZnO thin film, which consequently degraded the TFT performances. An optimal amount of crystalline water promotes an efficient conversion of ZnO precursor to ZnO semiconductor, thus yields high performance TFTs at low processing temperatures, and thereby enables low-cost and solution-processable printed electronics.

Introduction

Metal oxides for thin film transistors (TFTs) have gained increasing interests in past few years due to their high electron mobility, moderate processing temperature, high optical transparency, and so on.[1-6] Traditionally, metal oxide TFTs have been processed by vacuum deposition such as sputtering,[7] pulsed laser deposition,[8] and chemical vapor deposition.[9] These processes are costly for large area deposition and incompatible for plastic substrates due to high processing temperatures. Solution based deposition processes are desirable for simple to practice, easy to pattern, and scalable to large area.[10-14] Recent reports have shown that metal oxide based thin film semiconductor can be prepared from various soluble metal oxide precursors through the hydrolysis process.[15-17] The hydrolysis process is induced by incorporating an aqueous catalyst (acid or base) to the precursor solution before the thin film formation. The precipitation or metal oxide gel may be formed, during the hydrolysis, due to high reactivity of metal oxide precursors.[18] In contrast to hydrolysis, the non-hydrolyzed process requires high temperature calcinations, which cannot be accommodated by low thermal budget materials/processes.

Recent studies have shown that annealing metal oxides in humid environment (water vapor) enhanced TFT performance due to increased metal oxide formation.[18] Other studies discovered that water adsorption at the metal oxide semiconductor surface changed its conductivity and introduce hysteresis in TFTs.[19-20] Hence, it is important to quantify water effects in ZnO thin film formation (hydrolysis process), quality, and the ZnO TFT performance.

In this study, an in-depth investigation is conducted to reveal the effects of water incorporation in ZnO precursor solutions for ZnO thin film formation and its TFT device performance. Using water as an additive in ZnO precursor eliminates water vapor assisted annealing during the formation of ZnO thin film, and yields a simple in-situ hydrolysis process within the ZnO film. The TFTs are test vehicles for characterizing ZnO thin film semiconductor. The device environmental stability and voltage bias stability are studied to demonstrate the ZnO TFTs robustness for practical applications.

Experiment

The ZnO precursor solution is prepared by dissolving ZnO powders (Sigma Aldrich) in ammonium solution (Sigma Aldrich, 99%) to form 0.1 M ($Zn(NH_3)_4^{2+}$) complex, precursor, saturated solution. Different volume ratios of water (2%, 5%, 10%, 30%, and 50%) is added to the precursor solution and stirred overnight prior to use. TFT device is fabricated using a heavily doped p-type Si wafer (Silicon Quest International, Inc.) as the gate electrode/substrate and 200 nm of thermally grown SiO_2 as gate dielectric. Prior to spin coating the ZnO precursor solutions, the Si/SiO_2 substrates are cleaned with acetone, isopropyl alcohol (IPA), followed by Ar plasma treatment to facilitate the film formation on the substrate. The ZnO precursors are spun coated at 3000 rpm for 30 s to yield a ~10 nm thin film. The coated substrates are annealed at different temperature (150 ^oC or 250 ^oC) and environment conditions (dry annealing or water vapor assisted annealing). The Al electrodes, as source/drain, are deposited on the ZnO thin film with a shadow mask. For the TFT aging experiments, the nitrogen, vacuum, and 150^oC oven for 12

hrs conditions are used for performance comparison.

The transistors are characterized with Keithley 4200 semiconductor analyzer in vacuum, N_2 and ambient conditions for various studies. For each condition, a sampling size of 24-32 transistors is used. The field-effect mobility of ZnO TFTs is extracted using the following equation in the saturation region: $I_D = W/(2L)C_i\mu(V_G-V_T)^2$, where I_D is the drain current, μ is the field-effect mobility, C_i is the capacitance per unit area (SiO_2, 200 nm, C_i = 17 nF cm^{-2}), V_G and V_T are gate voltage and threshold voltage, and W/L are channel width/length (1000 μm/100 μm), respectively.

Surface properties of the ZnO film are characterized by two-dimensional X-ray diffraction (2D XRD) (Bruker-AXS D8 DISCOVER GADDS). The transmittance spectra of the ZnO films deposited on quartz substrates are measured using UV-Vis-NIR spectrophotometer (UV-3600 Shimadzu). The surface morphology and the roughness of the ZnO film deposited on a silicon substrate are studied by tapping-mode atomic force microscopy (TM-AFM) (Bruker ICON-PKG) and Field Emission Scanning Electron Microscope (FE-SEM) (JEOL JSM-7600F). X-ray photoelectron spectroscopy (XPS) (VG ESCALAB-220i XL) is for XPS spectra.

Result and Discussion

Thin film surface characterization

A 50 nm ZnO thin film on Si substrate is characterized by 2D XRD and the result is shown in Fig. 1a. The presence of weak diffraction peaks infers a weak Wurzite crystalline phase. The crystalline Wurzite structure with weak (002) orientation is further confirmed (Fig. S1) with a compressed ZnO nanoparticle sample.

Cite this: DOI: 10.1039/c0xx00000x

www.rsc.org/xxxxxx

ARTICLE

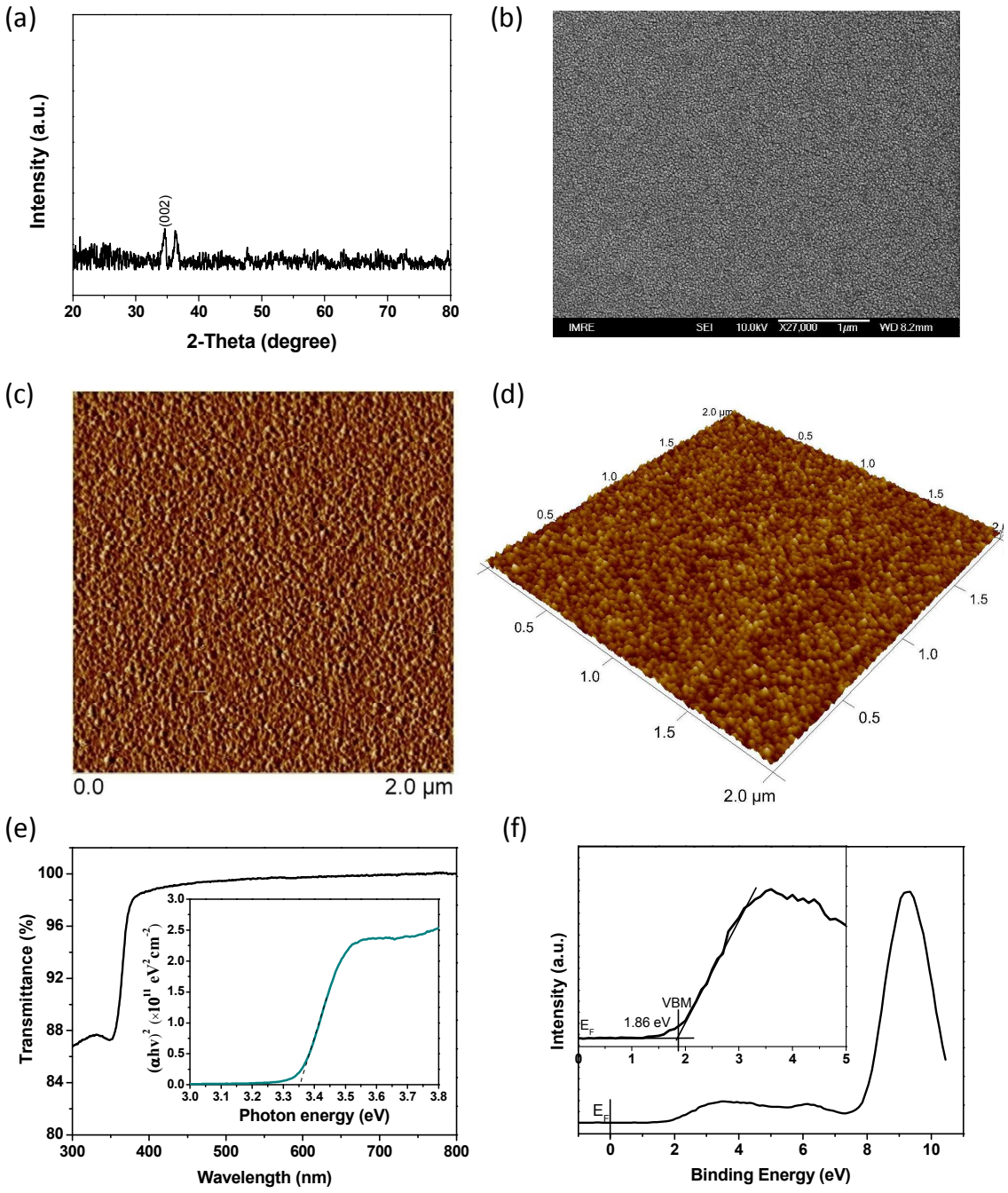

Fig. 1 (a) Two-dimensional XRD pattern of ZnO thin film annealed at 250 °C on silicon substrate. (b) The FESEM image of the ZnO thin film annealed at 250 °C on silicon substrate. (c-d) The phase and topography images 250 °C annealed ZnO thin film on silicon substrate. (e) Optical transmission spectra of the ZnO thin film on quartz substrate (Inset is the absorption coefficient as a function of photon energy). (f) Valence band spectrum of the ZnO thin film (Inset is the zoom-in image of the spectra near Fermi-energy of ZnO surface).

The ZnO surface morphology is studied using FESEM and tapping-mode AFM. The FESEM image shows a smooth surface with the crystal size in the nanometer range (Fig. 1b). This is further confirmed by tapping-mode AFM analysis. As shown in

Fig. 1c-1d, the phase and topography images reveal high quality thin film with surface roughness of 0.33 nm. The ZnO grain sizes are estimated to be about 6.2 nm from the AFM images. This grain size was believed to be beneficial to the mobility and adatom diffusion on the semiconductor surface.[21]

The optical transmission spectra of the ZnO thin film on quartz substrate is shown in Fig. 1e. From the transmittance spectra, the absorption coefficient as a function of photon energy is obtained. The thin film has good transparency in the visible region with corresponding optical band gap of 3.33~3.35 eV (inset) obtained using the Tauc model,[22] and the Davis Mott model[23] in the high absorbance region. The obtained optical band gap is similar to that of polycrystalline ZnO (3.37 eV).[24]

The valence band (VB) spectrum of the thin film is obtained by high resolution XPS, shown in Fig. 1f and the insert. From the zoomed-in spectrum near Fermi-energy at the ZnO film surface (the inset), the valence band maximum (VBM) of 1.86 eV (calibrated) is calculated.

XPS analysis is used to differentiate oxygen states in the ZnO thin films obtained from ZnO precursor solutions containing different water ratios. Fig. 2 displays the detailed C 1s and O 1s scans. There is no noticeable difference in peak shape and main peak position for the ZnO films annealed at 250 °C. The three O1s core level peaks under the broad shouldered oxygen peak can be assigned to a ZnO lattice peak (529.9 eV), ZnO lattice peak in the oxygen-deficient region (531.2 eV), and Zn hydroxide peak (532.1 eV).[25] For dry-annealed ZnO film with 0% water in the precursor, the metal hydroxides are about 14.0%, while the data obtained from ZnO film with 2% water incorporation only show 6.3% hydroxides at the same annealing conditions. By increasing water volume percentage to 50% in ZnO precursor, ZnO hydroxides are increased to 17% which is the result of the O-H bond in H_2O trapped in the bulk thin films. Higher hydroxide content means more defect sites, which deteriorate the charge carrier mobility resulting in poor TFT device performance. For C 1s core levels, the peak located at 284.6 eV, as a reference peak, is attributed to C-C and C-H moieties. The higher binding energy peaks can be assigned to carbon oxide groups.[26]

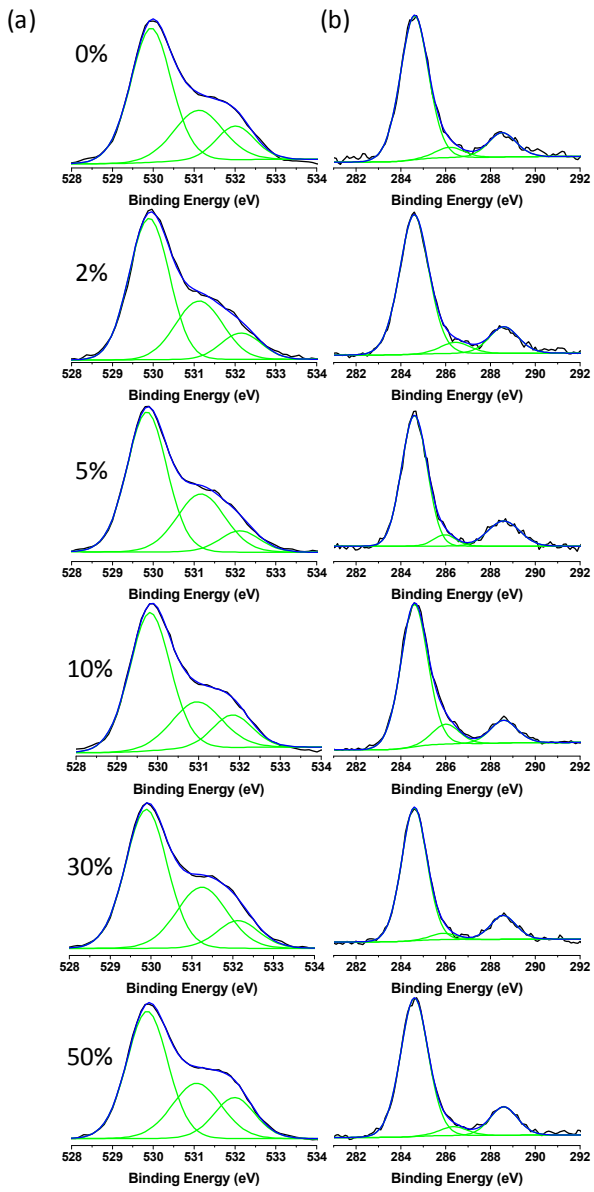

Fig. 2 O1s (a) and C1s (b) XPS spectra for annealed (at 250 °C) ZnO thin films with different water contents from volume ratio of 0% to 50% in the precursor solutions.

Thin film transistor characterization

The ZnO thin film transistor is a test vehicle for studying the semiconducting characteristics of the ZnO film. Figure 3a shows the TFT based on a bottom gate and top contact structure with typical channel length (L) and channel width (W) of 100 μm and 1000 μm, respectively. The TFT transfer curves measured by Keithley 4200 are shown in Fig. 3b-h. The TFTs exhibit excellent switch characteristics at given drain bias voltages. Figures 4a-g present statistics of field effect mobility (μ) of the ZnO TFTs at different water contents and different process conditions. Figure 4h summarizes the average mobility and the threshold voltage (V_T) with standard deviation for different precursor solutions. The ZnO film, with 0% water incorporation, after dry annealing at 250 °C resulted low TFT performances: low field effect mobility (1.2 $cm^2V^{-1}s^{-1}$) and high V_T shift (41-45V). With annealing temperature increased to 350 °C, the mobility of the

TFT device increases to 2.0 $cm^2V^{-1}s^{-1}$ (Fig. S2). When the ZnO film is annealed with present of water vapor at 250 °C, the TFT device mobility is 2.2 $cm^2V^{-1}s^{-1}$ with lower V_T shift (25-29 V): 80% increasing in mobility comparing to that of dry annealed devices at the same temperature. This is expected due to more efficient ZnO conversion from its hydroxides and further by electron donation of polar water molecules to enhance free carrier concentration and conductivity during the charge transfer between ZnO and water molecules ($H_2O(g) \rightarrow H_2O^+(ad) + e^-$).[18-19, S1] An illustration of this phenomenon is given in Fig. S3. Similarly, the thin films with 2% and 5% water have also resulted in good transistor performance with higher filed mobility (up to 1.8 $cm^2V^{-1}s^{-1}$) and relatively lower V_T shift. In addition, less hysteresis of transfer curves is observed due to less charge traps existed in the ZnO films (Fig. S4). When increasing water content further in the precursor solutions, the ZnO TFT performances are lower with decreased μ, increased V_T and turn-on voltage, summarized in Fig 4h. It is generally believed that the lower TFT performances are the result of increased trap density from excessive water in the ZnO film. The trap sites are formed during charge transport. The trap concentration can be estimated by the displacement of V_T ($N_{tr} = C_i\Delta V_T/e$), which is increased with increasing water content. In the case of 50% water content, the calculated trap concentration at the ZnO semiconductor and dielectric interface is 5.1×10^{12} cm^{-2}, the highest in the study. The positive V_T shift is the result of enhanced acceptor like traps from the extra water trapped in the ZnO thin films.[19] When testing the device in vacuum or N_2 environment, hysteresis diminishes as a result of the desorption of H_2O molecules from the ZnO film, thus reducing surface induced traps.

There are two experiments to quantify aging effects: 1) in the air with constant humidity (40%) for one week, and 2) in the vacuum or inert condition (water and oxygen free) for two weeks. With the devices are stored in the air, the V_T shift is toward the negative voltage direction and the off current is increased rapidly from 10^{-12} Amp to 10^{-8} - 10^{-9} Amp resulting in lower On/Off current ratio (Fig. S5). This was reported as surface-induced time-dependent instability effect.[27] When the devices are stored in the vacuum or inert environment, the ZnO TFTs from precursors with 2%-30% water show improved performances. The device mobility μ and threshold voltage V_T approach to their equilibrium values at 2.0-2.3 $cm^2V^{-1}s^{-1}$ and 23-30 V respectively. The turn-on voltage is around 0 V, shown in Fig 5. This is clearly evidence of 1) the conversion from Zn hydroxides (e.g. $Zn(OH)_2$) to ZnO has reached its equilibrium and 2) the extra water has been removed from ZnO film at the given extended time and environment conditions. In the case of TFTs made of ZnO precursors with 0% and 50% water, the devices exhibited lower performances even after aging in the vacuum or inert environment, which suggests that the defects introduced during the formation of the ZnO thin film are permanent: the lack of water during hydrolysis (0% water) and excessive water (50% water) incurring trapping sites in the ZnO thin film.

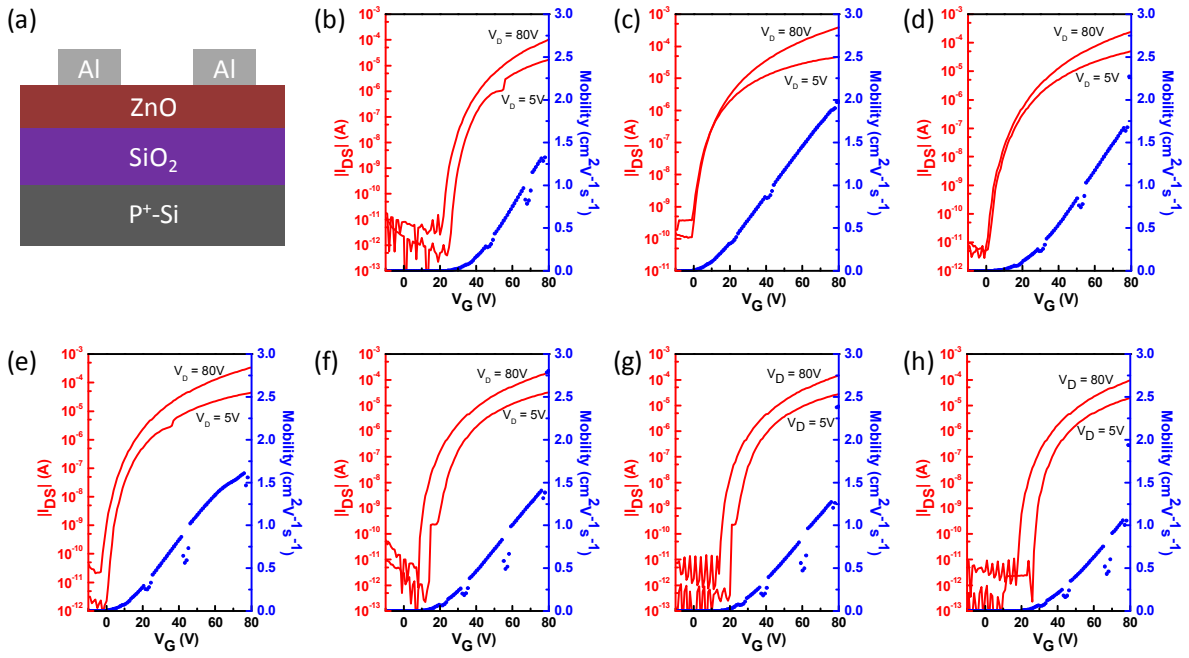

Fig. 3 (a) The device structure used in this study. (b-h) Transfer curves of ZnO TFTs fabricated with different conditions (dry annealing, water vapor annealing, water volume ratio of 2%, 5%, 10%, 30% and 50% in the precursor solutions, respectively). Red: drain current; blue: extracted field-effect mobility as a function of gate voltage. The transfer characteristics were acquired with a source–drain voltage of 5 V and 80 V.

Cite this: DOI: 10.1039/c0xx00000x

www.rsc.org/xxxxxx

ARTICLE

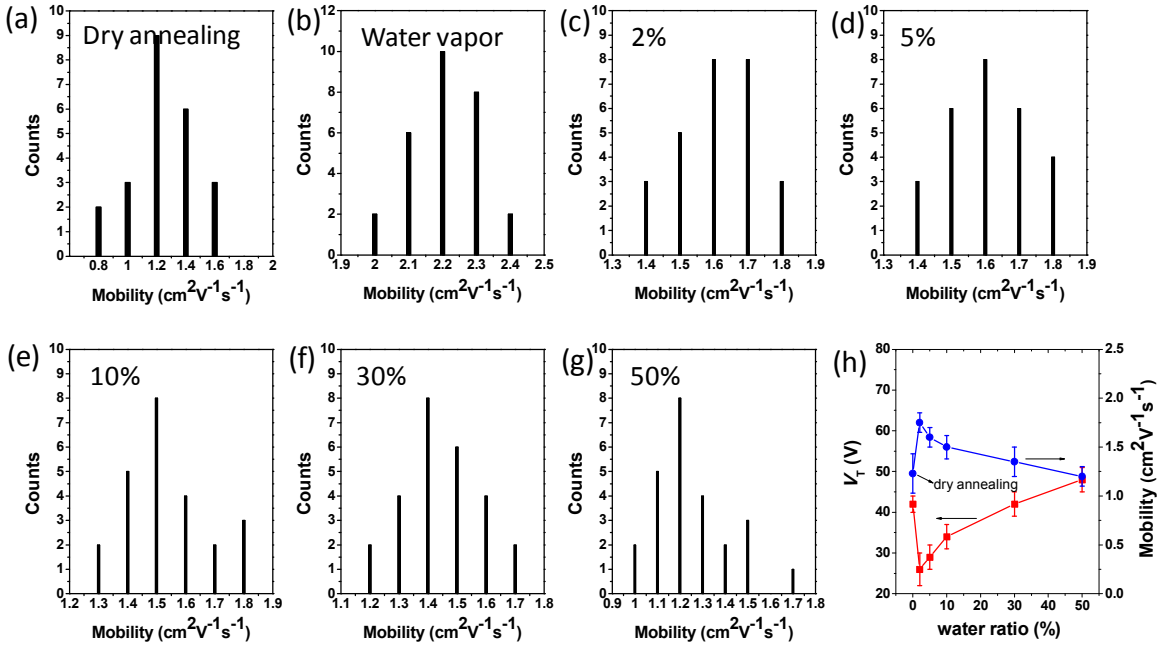

Fig. 4 (a-g) The statistical data of the mobility based on the ZnO thin film with different water ratio, (h) the V_T and mobility as a function of water ratio in the precursor solutions.

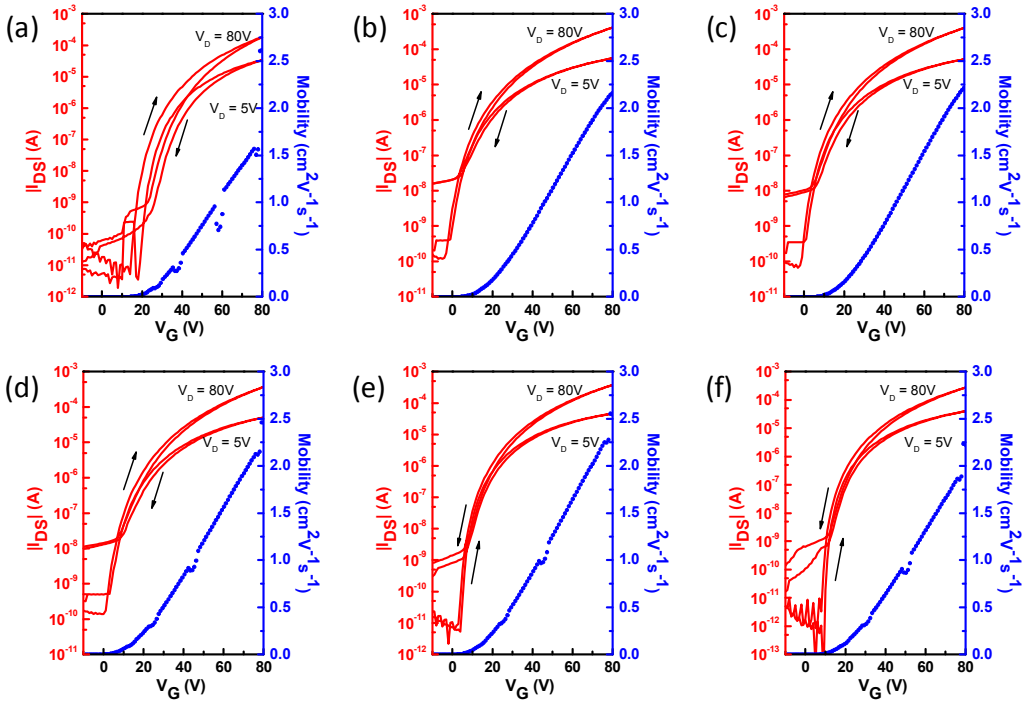

Fig. 5 The device stabilities of the ZnO thin film with different water ratio in the precursor solutions stored in N_2 for two weeks tested in ambient conditions (a: dry annealing, b-f: water volume ratio of 2%, 5%, 10%, 30% and 50%).

Table 1 Field-effect mobility (μ), threshold voltage (V_T), and current on/off ratio ($I_{on/off}$) of ZnO TFTs made from different ZnO precursor solutions and process conditions.

Water content	μ_{ave} [$cm^2V^{-1}s^{-1}$]	μ_{aged} [$cm^2V^{-1}s^{-1}$][a]	V_T [V]	I_{On}/I_{Off}
0%	1.2±0.4	1.5±0.2	41-45	10^6-10^7
Water vapor[b]	2.2±0.2	-	25-29	10^7-10^8
2%	1.7±0.2	2.3±0.1	27-31	10^7-10^8
5%	1.7±0.2	2.3±0.1	28-32	10^7-10^8
10%	1.5±0.2	2.2±0.1	34-38	10^7-10^8
30%	1.4±0.3	2.0±0.2	40-43	10^6-10^7
50%	1.2±0.4	1.9±0.2	46-50	10^6-10^7

a) TFT mobility after aging in N_2 conditions for two weeks. b) The device treated with water vapor during annealing.

The conversion mechanism from the ammonia–aqueous ZnO precursor solution to ZnO semiconductor is illustrated in Scheme 1.[28-29] When water is introduced into the precursor solution, the solution pH is decreased resulting in complex ($Zn(NH_3)_4^{2+}$) to Zn^{2+} and NH_4^+ ions deformation. Then the Zn^{2+} and OH^- react to form zinc hydroxide ($Zn(OH)_2$) which is easily decomposed to ZnO at about 100 °C.

1) $ZnO + 4NH_3(aq) + H_2O(l) \longrightarrow Zn(NH3)_4^{2+}(aq) + 2OH^-$

2) $\xrightarrow[pH\downarrow]{+4H_2O} Zn^{2+} + 4NH_4^+(aq) + 6OH^-$

3) $\longrightarrow Zn(OH)_2(s) + 4\ NH_3(g) + 4H_2O(l)$

4) $Zn(OH)_2 \xrightarrow{\triangle} ZnO(s) + H_2O(g)$

Scheme 1 Schematic description of the mechanism for ammonia-ZnO precusor solution.

When excessive water is introduced during the ZnO film formation, the water is adsorbed by the bulk thin film. These water molecules act as acceptor-like traps in the TFT source/drain channel, thus the trap density increased. As shown in Table 1, the V_T has changed from 27 V to 46 V when the water content increased from 2% to 50%, and the mobility has decreased from 1.8 $cm^2V^{-1}s^{-1}$ to 1.2 $cm^2V^{-1}s^{-1}$ accordingly. Therefore, only small amount of water, 1-2 % crystalline water, is sufficient to enhance the ZnO solubility in ZnO precursor solution and to promote the hydrolysis during the ZnO film formation.

The low temperature processability of ZnO has been evaluated in this study. A set of experiments are designed to investigate the annealing temperature and subsequent aging effects on the TFTs performances. Fig. 6a-b shows typical I_{DS}-V_G transfer characteristics and field effect mobility for TFTs fabricated using ZnO semiconducting film casted by ZnO precursor with 2% water and annealed at 150 °C. The devices are characterized again after 12 hrs storage in vacuum or nitrogen environment. The average mobility obtained from the low temperature annealed TFT devices is 0.15 $cm^2V^{-1}s^{-1}$, comparing to 1.76 $cm^2V^{-1}s^{-1}$ of same configured device annealed at 250 °C. The reduced mobility is the result of incomplete ZnO lattice formation at 150 °C. It is worth notice that the low temperature processed TFTs exhibit very good electrical field response, e.g. excellent saturation characteristics and large I_{on}/I_{off} ratio. After the device stored in the nitrogen or vacuum environment for 12 hrs, the device performances increase more than 2× due to water desorption resulting the reduction of traps density (Fig. 6b). The extended thermal annealing at 150 °C for 12 hrs gives even higher TFT performances (μ = 0.36 $cm^2V^{-1}s^{-1}$) due to continuous ZnO conversion at the extended annealing time at the elevated temperature. The performance of the ZnO TFT annealed at 150 °C in this study is higher than most n-type TFTs (organic and inorganic) processed at similar temperature. Therefore, the lower temperature conversion of Zn hydroxide to ZnO using the proposed ZnO precursors with calculated water content can enable the low cost printed electronics applications.

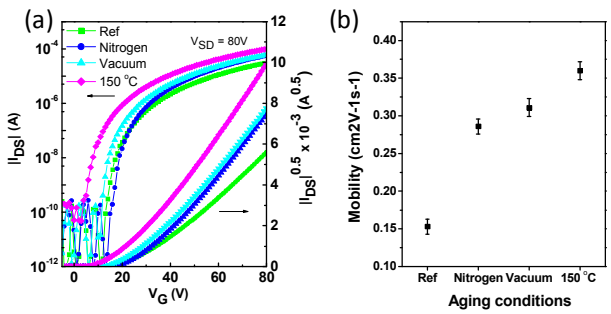

Fig. 6 (a-b) The transfer and output characteristics of ZnO TFTs at annealing temperature of 150 °C test in N_2 conditions.

The operational stability of ZnO thin film transistors is evaluated with on/off cycle test and bias stress test. As shown in Fig. 7a,c, the TFT annealed at the present of water vapor results near constant current during the on/off cycle (Fig.7a) and almost no hysteresis and V_T shift (Fig. 7c). However, as shown in Fig. 7b, d, the TFT with 10% or more water content results decreased on-current during the on/off cycles (Fig. 7b) and drafted threshold voltage under the positive voltage stress (Fig. 7d), which indicate the existence of the bulk traps by excessive water in the ZnO semiconductor film.

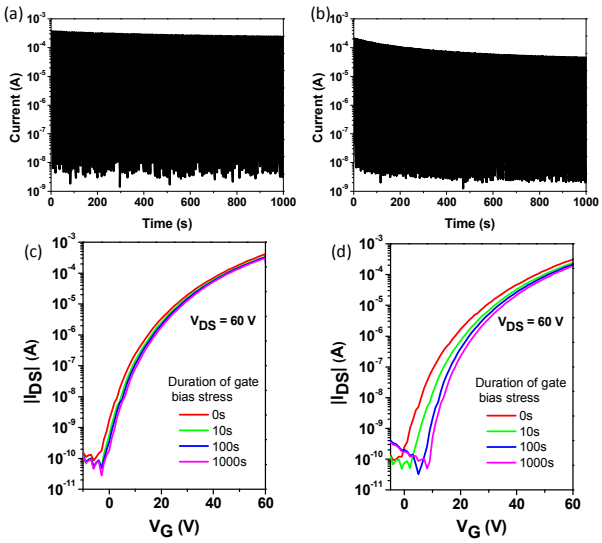

Fig. 7 Dynamic stress test of a ZnO TFT with water vapor annealing (a) and 10% water content in the precursor solutions (b) during continuous cycling between ON (V_G = 60 V) and OFF (V_G = 0 V) states; bias stress test of the ZnO TFT with water vapor annealing (c) and 10% water content in the precursor solutions (d) with + 20 V bias.

Conclusions

In summary, this study investigated ZnO semiconducting film formation and ZnO TFT performances through hydrolyzing ZnO precursors with different water concentration. It was found that introducing controlled amount of water molecules, either in the form of water vapor during annealing or as an additive in the ZnO precursor solutions, has enhanced the ZnO thin film quality by improving the yield of polycrystalline ZnO from its hydroxides. However, excessive amount of water molecules in the ZnO precursor was undesirable due to the formation of acceptor-like traps in ZnO thin film, led to lower TFT mobility, greater V_T shift and hysteresis voltage, thus degrading TFT performances. In addition, this study has also found that the water vapor or the optimal amount of crystalline water promoted ZnO hydrolysis at low temperature (as low as 150 °C) and resulted in desirable performances of the ZnO thin film transistors. The low temperature processability of the ZnO precursor enablers many low cost printed and flexible electronics applications.

Notes and references

[a]*Department of Chemistry, National University of Singapore, 3 Science Drive 3, 117543, Singapore. Fax: +65 6779 1691; Tel: +65 6516 2677 Email: chmwuj@nus.edu.sg*
[b]*Institute of Materials Research and Engineering, A*STAR, 3 Research Link, Singapore 117602, Singapore. wuj@imre.a-star.edu.sg and zhangj@imre.a-star.edu.sg*

Acknowledgment

This work was financially supported by MOE Tier 2 grant (MOE2011-T2-2-130), IMRE Core Funding (IMRE/12-1P0902), and A*STAR SERC TSRP grant (Grant #102 170 0137).

1 K. Nomura, H. Ohta, A. Takagi, T. Kamiya, M. Hirano and H. Hosono, *Nature*, 2004, **432**, 488.
2 H. Yabuta, M. Sano, K. Abe, T. Aiba, T. Den, H. Kumoni, K. Nomura, T. Kamiya, and H. Hosono, *Appl. Phys. Lett.*, 2006, **89**, 112123.
3 H. Q. Chiang, J. F. Wager, R. L. Hoffman, J. Jeong, and D. A. Keszler, *App. Phys. Lett.*, 2005, **86**, 013503.
4 N. L. Dehuff, E. S. Kettenring, D. Hong, H. Q. Chiang, J. F. Wager, R. L. Hoffman, C. H. Park, and D. A. Keszler, *J. Appl. Phys.*, 2005, **97**, 064505.
5 T. Moriga, D. R. Kammler, and T. O. Mason, *J. Am. Ceram. Soc.*, 1999, **82**, 2705.
6 H. S. Kim, M.-G. Kim, Y.-G. Ha, M. Kanatzidis, T. J. Marks, and A. Facchetti, *J. Am. Chem. Soc.*, 2009, **131**, 10826.
7 P. F. Carcia, R. S. McLean, M. H. Reilly, and G. Nunes, *Appl. Phys. Lett.*, 2003, **82**, 1117.
8 J. Nishii, F. M. Hossain, A. Takagi, T. Aita, K. Saikusa, Y. Ohmaki, I. Ohkubo, S. Kishimoto, A. Ohtomo, T. Fukumura, F. Matsukura, Y. Ohno, H. Koinuma, H. Ohno, and M. Kawasaki, *Jpn. J. Appl. Phys.*, 2003, **42**, 347.
9 J. Jo, O. Seo, H. Choi, and B. Lee, *Appl. Phys. Express*, **2008**, **1**, 041202.
10 Y.-J. Chang, D.-H. Lee, G. S. Herman, and C.-H. Chang, *Electrochem. Solid-State Lett.*, 2007, **10**, 135.
11 B. Norris, J. Anderson, J. F. Wager, and D. A. Keszler, *J. Phys. D: Appl. Phys.*, 2003, **36**, 105.
12 B. S. Ong, C. S. Li, Y. N. Li, Y. L. Wu, and R. J. Loutfy, *J. Am. Chem. Soc.*, 2007, **129**, 2750.
13 D. Paraguay, L. Estrada, N. Acosta, E. Andrade, and M. Miki-Yoshida, *Thin Solid Films*, 1999, **350**, 192.
14 S. A. Studenikin, N. Golego, and M. Cocivera, *J. Appl. Phys.*, 1998, **83**, 2104.
15 S. T. Meyers, J. T. Anderson, C. M. Hung, J. Thompson, J. F. Wager, and D. A. Keszler, *J. Am. Chem. Soc.*, 2008, **130**, 17603.
16 S. K. Park, Y. H. Kim, and J. I. Han, *J. Phys. D: Appl. Phys.*, 2009, **42**, 125102.
17 D. H. Lee, Y. J. Chang, G. S. Herman, and C. H. Chang, *Adv. Mater.*, 2007**, 19**, 843.
18 K. K. Banger, Y. Yamashita, K. Mori, R. L. Peterson, T. Leedham, J. Rickard, and H. Sirringhaus, *Nat. Mater.*, 2011, **10**, 45.
19 J. Park, J. K. Jeong, H. J. Chung, Y. J. Mo, and H. D. Kim, *Appl. Phys. Lett.*, 2008, **92**, 072104.
20 M. Fakhri, H. Johann, P. Gorrn, T. Riedl, *ACS Appl. Mater. Interfaces*, 2012, **4**, 4453.
21 G. Adamopoulos, A. Bashir, W. P. Gillin, S. Georgakopoulos, M. Shkunov, M. A. Baklar, N. Stingelin, D. D. C. Bradley, and T. D. Anthopoulos, *Adv. Funct. Mater.*, 2011, **21**, 525.
22 J. Tauc, Amorphous and Liquid Semiconductors (Plenum, London, 1974).
23 E. A. David, and N. F. Mott, *Philos. Mag.*, 1970, **22**, 903.
24 V. Srikant, and D. R. Clarke, *J. Appl. Phys.*, 1998, **83**, 5447.
25 P. K. Biswas, A. De, L. K. Dua, and L. Chkoda, *Bull. Mater. Sci.*, 2006, **29**, 323.
26 C. Donley, D. Dunphy, D. Panie, C. Carter, K. Nebesny, P. Lee, D. Alloway, and N. R. Armstrong, *Langmuir*, 2002, **18**, 450.
27 K. -T. Kim, K.Lee, M. S. Oh, C. H. Park, and S. Im, *Thin solid film*, 2009, **517**, 6345.
28 S. Yamabi, and H. Imai, *J. Mater. Chem.*, 2002, **12**, 3773.

29 K. Kim, S. Y. Park, K. -H, Lim, C. Shin, J. -M Myoung, and Y. S. Kim, *J. Mater. Chem.*, 2012, **22**, 23120.